HHS Public Access

Author manuscript

Nat Immunol. Author manuscript; available in PMC 2016 November 23.

Published in final edited form as:

Nat Immunol. 2016 July ; 17(7): 834–843. doi:10.1038/ni.3461.

Id2 reinforces T_H1 cell differentiation and inhibits E2A to repress T_{FH} cell differentiation

Laura A. Shaw[1,6], **Simon Bélanger**[2,6], **Kyla D. Omilusik**[1], **Sunglim Cho**[1], **James P. Scott-Browne**[3], **J. Philip Nance**[2], **John Goulding**[1], **Anna Lasorella**[4], **Li-Fan Lu**[1], **Shane Crotty**[2,5,*], and **Ananda W. Goldrath**[1,*]

[1]Department of Biological Sciences, University of California San Diego, La Jolla, CA

[2]Division of Vaccine Discovery, La Jolla Institute, La Jolla, CA

[3]Division of Signaling and Gene Expression, La Jolla Institute, La Jolla, CA

[4]Institute for Cancer Genetics, Columbia University Medical Center, New York, NY

[5]Department of Medicine, University of California San Diego, La Jolla, CA

Abstract

Differentiation of T helper (T_H) effector subsets is critical for host protection. E protein transcription factors and Id proteins are important arbiters of T cell development, but their role in differentiation of T_H1 and T_{FH} cells is not well understood. T_H1 cells showed robust Id2 expression compared to T_{FH} cells, and RNAi depletion of Id2 increased T_{FH} cell frequencies. Further, T_H1 cell differentiation was blocked by Id2 deficiency, leading to E protein-dependent accumulation of effector cells with mixed characteristics during viral infection and severely impaired generation of T_H1 cells following *Toxoplasma gondii* infection. The T_{FH}-defining transcriptional repressor Bcl6 bound the *Id2* locus, providing a mechanism for the bimodal Id2 expression and reciprocal development of T_H1 and T_{FH} cell fates.

Introduction

Recognition of a pathogen by the immune system initiates a multi-step transcriptional program which directs $CD4^+$ T cell differentiation into distinct T helper populations (T_H) that coordinate eradication of infection. T_H1 effector cells secrete inflammatory cytokines

*Co-corresponding author: Correspondence should be addressed to A.W.G. (agoldrath@ucsd.edu) or S.C. (shane@lji.org). Telephone: 858-534-5839 (A.W.G.) or 858-752-6818 (S.C.).

[6]These authors contributed equally to this work.

AUTHOR CONTRIBUTIONS

L.A.S. and S.B. performed experiments; K.D.O., J.P.S-B., J.P.N., Su.C., J.G., L-F.L. and A.L. provided intellectual input and generated new reagents or performed experiments; L.A.S., S.B., S.C. and A.W.G. conceived the study, analyzed and interpreted data, and wrote the manuscript.

COMPETING FINANCIAL INTERESTS

The authors declare no competing financial interests.

ACCESSION CODE

Gene Expression Omnibus: Microarray data have been deposited under accession code GSE74854.

and activate immune cells[1]. Follicular helper (T_{FH}) cells secrete cytokines and upregulate ligands that induce B cells to form germinal centers, class switch, and generate high-affinity antibodies[2]. Differentiation of $CD4^+$ T cells is directed by cytokine-induced activation of STAT proteins and lineage determining transcription factors such as T-bet and Bcl6[3]. Following activation, T_H1 cells receive signals that initiate T-bet expression and induce migration from the lymphoid tissues to infected or inflamed areas of the body[1]. In contrast, to properly differentiate, T_{FH} cells must upregulate Bcl6 and the chemokine receptor CXCR5 allowing movement from the T cell zone into the B cell follicle[2]. The differentiation of T_H1 and T_{FH} cells is interconnected through antagonistic interplay between T-bet and Bcl6, and Bcl6 and Blimp-1[4–8].

E protein transcription factors and their natural repressors, the inhibitor of DNA binding (Id) proteins, play a crucial role in the differentiation of numerous lymphocyte populations such as B cells, innate lymphoid cells, natural killer cells, invariant NKT cells, αβ γδ and $CD8^+$ effector and memory T cells[9–17]. Recently, studies have highlighted the role played by Id2, Id3 and E proteins in mature $CD4^+$ T cells, particularly in the differentiation and maintenance of regulatory T (T_{reg}) cells and T_H17 cells[18–21]. Deletion of E proteins leads to an increase in T_{reg} cell populations; however, deletion of Id2 and Id3 cripples the differentiation and localization of $Foxp3^+$ T_{reg} cells[18,20]. Additionally, Id2-deficient $CD4^+$ T cells were unable to mount a robust T_H17 response in a mouse model of experimental autoimmune encephalomyelitis[21]. Ectopically expressed basic helix-loop-helix (bHLH) transcription factor achaete-scute homolog 2 (Ascl2) binds E-box sites to drive upregulation of CXCR5 *in vitro*, resulting in augmented accumulation of $CD4^+$ T cells in the B cell follicle *in vivo*[22]. However, Ascl2 did not induce Bcl6, raising the question of how E protein activity and the induction of CXCR5 and Bcl6 are interrelated. Furthermore, our own studies have shown differential Id2 and Id3 mRNA expression in T_H1 and T_{FH} cells[23]. Thus, we further explored the biology of Id2 and Id3 in the differentiation of T_H1 and T_{FH} during infection.

Results

Id2 and Id3 define T_H1 and T_{FH} effector $CD4^+$ T cell subsets

We determined the abundance of Id2 and Id3 in $CD4^+$ T cell subsets by using reporter mice in which cDNA encoding for yellow fluorescent protein (YFP) or green fluorescent protein (GFP) were inserted in the *Id2*[14] or *Id3*[24] gene, respectively. We crossed both lines to SMARTA TCR transgenic mice (LCMV-specific, gp66-77 IA^b-restricted) to generate $Id2^{YFP/+}$ and $Id3^{GFP/+}$ SMARTA $CD4^+$ T cells, which were transferred into B6 hosts that were then infected with LCMV-Armstrong. T_H1 and T_{FH} differentiation was assessed in Id2-YFP^{lo} and Id2-YFP^{hi} subsets following infection. In parallel, we infected $Id2^{YFP/+}$ or $Id3^{GFP/+}$ mice with LCMV to follow polyclonal $CD4^+$ T cell differentiation. We observed that Id2-YFP^{lo} cells were almost exclusively T_{FH} cells ($CXCR5^+SLAM^{lo}$ or $CXCR5^+PD\text{-}1^{lo}$) and GC T_{FH} ($CXCR5^+PD\text{-}1^+$), while the vast majority of Id2-YFP^{hi} cells displayed a T_H1 phenotype ($SLAM^+CXCR5^-$ or $CXCR5^-PD\text{-}1^-$) (Fig. 1a, Supplementary Fig. 1a). Similarly, we found that Id3 expression was highly polarized: Id3-GFP^{lo} cells

enriched in the T_H1 population and Id3-GFP^{hi} cells enriched in T_{FH} and GC T_{FH} populations (Fig. 1b, Supplementary Fig. 1b).

We also generated *Id2*$^{YFP/+}$*Id3*$^{GFP/+}$ dual reporter mice and analyzed coordinate Id2 and Id3 expression after LCMV infection. Naive CD4$^+$ T cells expressed intermediate and high amounts of Id2 and Id3, respectively. After infection, T_H1 cells showed a substantial increase in Id2-YFP expression compared to naive cells (Fig. 1c). In contrast, T_H1 cells lost Id3-GFP expression, and T_{FH} cells maintained high expression of Id3-GFP (Fig. 1c). Compared to T_{FH} cells, GC T_{FH} cells had equivalent expression of Id3-GFP reporter (data not shown). Histology revealed that the majority of Id2-YFP expressing CD4$^+$ T cells were excluded from the B cell follicle and germinal center (Fig. 1d). Our results show that Id2 and Id3 have contrasting expression patterns in T_H1 and T_{FH} cells following acute LCMV infection.

Impaired *Id2* expression enhances T_{FH} differentiation

To determine if differential *Id2* expression in CD4$^+$ T cells influences CD4$^+$ T cell differentiation *in vivo*, we expressed an shRNAmir specific for *Id2* (sh*Id2*) or a control shRNAmir (shCtrl) in SMARTA CD4$^+$ T cells, transferred cells into B6 mice, and analyzed T cell differentiation after LCMV infection. Expression of sh*Id2* in SMARTA CD4$^+$ T cells reduced *Id2* mRNA expression (Supplementary Fig. 2a). Among sh*Id2*$^+$ cells, there was an increased frequency of T_{FH} cells and decreased frequency of T_H1 cells compared to shCtrl (Fig. 2a–c). The bias was predominantly attributed to GC T_{FH} cells, identified as CXCR5$^+$Bcl6$^+$ cells (Fig. 2d–f) or CXCR5$^+$PSGL-1^{lo} (Supplementary Fig. 2c–e). We then examined the differentiation of sh*Id2*$^+$ cells earlier after infection (Supplementary Fig. 2f) and observed an increased frequency of CXCR5$^+$Bcl6$^+$ T_{FH} and a decreased T_H1 (CXCR5$^-$ Bcl6$^-$) population among sh*Id2*$^+$ cells (Fig. 2g–i). Analysis of early T_{FH} cells (CXCR5$^+$CD25$^-$)[25,26] also revealed an increased proportion among sh*Id2*$^+$ cells (Supplementary Fig. 2g–i). Thus, impaired Id2 expression appears to favor T_{FH} differentiation.

To examine B cell help by sh*Id2*$^+$ CD4$^+$ T cells we transferred sh*Id2*$^+$ or shCtrl$^+$ OT-II CD4$^+$ cells into *Bcl6*$^{fl/fl}$ CD4-Cre$^+$ mice[27], followed by immunization with NP-OVA in alum. After immunization, more sh*Id2*$^+$ T cells had differentiated into CXCR5$^+$PD-1$^+$ or CXCR5$^+$Bcl6$^+$ GC T_{FH} than control cells (Supplementary Fig. 2j,k). Increased frequencies of GC B cells (Fig. 2k) and plasma cells (Fig. 2l) were observed in sh*Id2*$^+$ recipients compared to control, with no differences in the NP-specific IgG titers (Fig. 2m), despite slightly reduced accumulation of sh*Id2*$^+$ CD4$^+$ T cells (Fig. 2j). Thus, Id2 expression appears to negatively impact T_{FH} cell differentiation.

Id2 is necessary for generation of T_H1 cells during infection

We next asked how the total absence of Id2 affects CD4$^+$ T cell differentiation. We crossed *Id2*-floxed (*Id2*$^{fl/fl}$) mice[28] to SMARTA TCR- and CD4-Cre transgenic lines to generate *Id2*$^{fl/fl}$CD4-Cre$^+$ SMARTA (*Id2*$^{-/-}$) mice in which *Id2* is deleted in αβ thymocytes. Naive *Id2*$^{-/-}$ SMARTA cells were CD44^{low} and indistinguishable from *Id2*$^{+/+}$ cells (data not shown). We transferred naive *Id2*$^{+/+}$ CD4-Cre$^+$ SMARTA (*Id2*$^{+/+}$) or *Id2*$^{-/-}$ cells into B6

hosts and followed their differentiation after infection. *Id2*$^{-/-}$ cells did not form a distinct T_H1 population (Fig. 3a,b, Supplementary Fig. 3a). Loss of T_H1 differentiation by *Id2*$^{-/-}$ cells was accompanied by decreased granzyme B, T-bet and IFNγ expression, and increased TCF-1 expression (Supplementary Fig. 3b,c). Notably, a prominent SLAM^{mid}CXCR5^{mid} population emerged among *Id2*$^{-/-}$ effector CD4$^+$ T cells, which was not observed in *Id2*$^{+/+}$ cells (Fig. 3a,b). This phenotype was also apparent in a polyclonal CD4$^+$ T cell response (Supplementary Fig. 3d). These results show that *Id2* is required for differentiation of T_H1 cells.

To understand the dysregulation of *Id2*$^{-/-}$ T_H1 cells, we further characterized the phenotypes of the *Id2*$^{-/-}$ populations after LCMV infection. *Id2*$^{+/+}$ and *Id2*$^{-/-}$ T_H1 cells maintained high expression of PSGL-1 and IL-2Rα, which both need to be downregulated for proper T_{FH} differentiation[25,29–31] (Fig. 3c,d). Analysis of the SLAM^{mid}CXCR5^{mid} population revealed that *Id2*$^{-/-}$ cells shared a partial phenotype with T_H1 cells, including high expression of PSGL-1, Ly6C and IL-2Rα, and were Bcl6^{low} when compared to *Id2*$^{+/+}$ or *Id2*$^{-/-}$ T_{FH} cells (Fig. 3c,d). Bcl6 expression was normal in sh*Id2*$^+$ early T_H1 and T_{FH} (Supplementary Fig. 3e) suggesting that partial loss of *Id2* does not impact T_H1 cell phenotype. In contrast, the complete absence of *Id2* impacted CD4$^+$ T cells throughout differentiation, permanently disrupting T_H1 cells.

Id2$^{-/-}$ cells were then assessed for their ability to support B cell responses. Eight days after LCMV infection of *Bcl6*$^{fl/fl}$ CD4-Cre$^+$ mice that had received *Id2*$^{+/+}$ or *Id2*$^{-/-}$ cells, we observed an increased frequency of *Id2*$^{-/-}$ T_{FH} cells, but their numbers were similar (Supplementary Fig. 3f). Plasma cell frequencies and anti-LCMV IgG titers in the serum were unchanged (Fig. 3e,f). However, GC B cell development was impaired in mice that received *Id2*$^{-/-}$ cells (Fig. 3e), suggesting that *Id2*$^{-/-}$ T_{FH} cells may have impaired function.

To further characterize the differentiation status of *Id2*$^{-/-}$ CD4$^+$ T cells outside the limitations imposed by 2-parameter flow cytometric plots, and because many of the *Id2*$^{-/-}$ cells could not be unambiguously assigned to either T_H1 or T_{FH} based on SLAM or CXCR5 expression**,** we employed viSNE multi-parameter clustering, where the overall position of each cell reflects similarity to neighboring cells or dissimilarity to non-neighboring cells based on expression of CD4, CD45.1, SLAM, CXCR5, Bcl6, TCF-1, PD-1 and T-bet[32]. We observed two geographically distinct populations in total CD4$^+$ or specifically in SMARTA CD4$^+$ T cells that uniquely expressed the T_H1 and T_{FH} markers SLAM and Bcl6, respectively (Fig. 3g). *Id2*$^{+/+}$ and *Id2*$^{-/-}$ T_{FH} populations are similar in location and appearance (Fig. 3g). However, *Id2*$^{-/-}$ T_H1 cells were located outside of the T_H1 multiparameter gate defined by *Id2*$^{+/+}$ T_H1 cells (Fig. 3g), further suggesting that Id2 is required for proper T_H1 differentiation.

To examine the defect of T_H1 differentiation in Id2-deficient cells, we employed a model of *Toxoplasma gondii* (*T. gondii)* infection for which the role of IFNγ-mediated T_H1 responses for long-term resistance and control of infection is well established[33]. *Id2*$^{fl/fl}$ CD4-Cre$^+$ mice infected with *T. gondii* harbored CD4$^+$ T cells with markedly reduced expression of both IFNγ and T-bet in the lamina propria of the small intestine compared to *Id2*$^{+/+}$ CD4-Cre$^+$ controls (Fig. 3h). No significant alteration in the frequencies of Foxp3$^+$ T_{reg} cells could be

detected (Fig. 3h). Thus in two distinct infections, we observe a severe loss of T_H1 effector T cells.

Id3 restrains T_{FH} differentiation

A second inhibitor of E protein activity, Id3, is chiefly expressed by T_{FH} and GC T_{FH} cells following infection and has been implicated as an inhibitor of T_{FH} differentiation. However, the role for Id3 in the generation of T_{FH} cells was not examined in the context of infection[22]. Thus, we generated *Id3*-floxed[34] CD4-Cre$^+$ SMARTA transgenic mice (*Id3*$^{-/-}$), transferred cells into B6 mice, and infected with LCMV. In response to infection, *Id3*$^{-/-}$ cells displayed an increased propensity to become both T_{FH} and GC T_{FH} when compared to *Id3*$^{+/+}$ cells (Supplementary Fig. 4a). Further, an increase in frequency of GC T_{FH} was also observed in polyclonal Id3-deficient CD4$^+$ T cells (Supplementary Fig. 4b). We next investigated whether constitutive expression of Id3 could inhibit T_{FH} differentiation; Id3-RV$^+$ or GFP-RV$^+$ LCMV NP-specific (NIP) CD4$^+$ T cells[35] were transferred into B6 mice, which were infected with LCMV. The acquisition of both T_{FH} (Supplementary Fig. 4c) and early T_{FH} (Supplementary Fig. 4d) characteristics were abrogated when Id3 was overexpressed. This is consistent with the observation that Id3 inhibited T_{FH} differentiation following protein immunization[22].

Loss of Id2 regulates expression of key T_H genes

To understand how Id2 impacts T_H1 and T_{FH} cell differentiation, we studied the global transcriptional changes in CD4$^+$ T cells resulting from *Id2* deficiency. *Id2*$^{+/+}$ and *Id2*$^{-/-}$ (encompassing both SLAM^{hi}CXCR5$^-$ and SLAM^{mid}CXCR5^{mid} populations) T_H1 and *Id2*$^{+/+}$ and *Id2*$^{-/-}$ CXCR5$^+$SLAM^{lo} T_{FH} cells were used for comparative gene expression profiling (Fig. 4a). Differential expression of T_H1- and T_{FH}-associated genes was confirmed for *Id2*$^{+/+}$ T_H1 and T_{FH} cells (Fig. 4b). We then compared gene expression profiles of *Id2*$^{+/+}$ and *Id2*$^{-/-}$ T_H1 cells and observed downregulation of T_H1-associated genes (*Gzmb*, *Slamf1* and *Cxcr6)* in the context of *Id2* deficiency, while genes associated with the T_{FH} program (*Cxcr5*, *Il6ra* and *Tcf7*) were upregulated (Fig. 4c). However, *Bcl6, Ascl2, Pdcd1* and *Icos*, all highly expressed by T_{FH} cells and important in T_{FH} differentiation, were not elevated in the *Id2*$^{-/-}$ T_H1 population when compared to *Id2*$^{+/+}$ T_H1 cells, indicating that E proteins control the expression of only a portion of T_{FH} signature genes (Fig. 4d).

We next characterized the impact of *Id2* deficiency on the expression of T_H1-associated genes. A T_H1 gene set was selected as all genes upregulated ≥1.4 fold in *Id2*$^{+/+}$ T_H1 cells compared to *Id2*$^{+/+}$ T_{FH} cells (Fig. 4b, green). *Id2*$^{-/-}$ T_H1 cells had reduced expression for ~78% of the T_H1-associated genes (Fig. 4e). Additionally, of the 144 genes most substantially downregulated in *Id2*$^{-/-}$ T_H1 cells compared to *Id2*$^{+/+}$ T_H1 cells (Fig. 4c, purple), ~79% were expressed at higher levels in *Id2*$^{+/+}$ T_H1 compared to *Id2*$^{+/+}$ T_{FH} cells (Fig. 4f). Thus, deletion of *Id2* impaired acquisition of the T_H1 program.

A T_{FH} gene set was defined as all genes expressed ≥1.4 fold in *Id2*$^{+/+}$ T_{FH} cells compared to *Id2*$^{+/+}$ T_H1 cells (Fig. 4b, blue). *Id2*$^{-/-}$ T_H1 cells inappropriately upregulate ~69% of the T_{FH}-associated genes (Fig. 4g). Analysis of genes most upregulated in *Id2*$^{-/-}$ T_H1 cells compared to *Id2*$^{+/+}$ T_H1 cells (Fig. 4c, grey) revealed that ~65% were preferentially

expressed in *Id2*$^{+/+}$ T_{FH} cells (Fig. 4h). These analyses indicate a substantial bias towards the T_{FH} gene expression program in *Id2*$^{-/-}$ T_H1 cells. When gene expression of *Id2*$^{+/+}$ and *Id2*$^{-/-}$ T_{FH} cells was contrasted, only 140 genes showed significant differential expression, indicating that established T_{FH} cells, which express lower levels of *Id2*, were moderately impacted by *Id2* deficiency (Fig. 4i).

The absence of proper T_H1 development in *Id2*$^{-/-}$ cells suggests that unchecked E2A activity impaired T_H1 differentiation. Analysis of genes differentially expressed between *Id2*$^{+/+}$ T_H1 and T_{FH} cells revealed a larger number of E2A-bound genes were upregulated in *Id2*$^{-/-}$ T_H1 cells compared to *Id2*$^{+/+}$ T_H1 cells (Fig. 4d), consistent with Id2 inhibition of E2A. We compared changes in gene expression with a list of E2A-target genes[16] and found that 62% of the genes upregulated in *Id2*$^{-/-}$ T_H1 cells are targets of E2A (Fig. 4j). These results suggest that Id2 is important for the maintenance of T_H1 gene-expression program and that its absence results in acquisition of a partial T_{FH} program.

E proteins drive CXCR5 expression

Our microarray results suggest that Id2 and E proteins act together to control CD4$^+$ T cell differentiation in part by regulating CXCR5 and expression of T_H1 effector molecules such as SLAM. We hypothesized that diminished E2A levels could rescue the defect observed in *Id2*-deficient cells. We expressed an shRNA targeting *Tcf3* (encoding E2A) or a control shRNA in *Id2*$^{+/+}$ and *Id2*$^{-/-}$ SMARTA CD4$^+$ T cells (Supplementary Fig. 5a). Cells were adoptively transferred into B6 mice infected the previous day, and differentiation of the transferred cells was analyzed. As expected, *Id2*$^{-/-}$ cells expressing control shRNA could not correctly differentiate into T_H1 cells (Fig. 5a). However, *Id2*$^{-/-}$ T_H1 cells were rescued by sh*Tcf3* expression and defects in SLAM and CXCR5 expression were both corrected (Fig. 5a). Thus, the defective T_H1 differentiation we observe in the absence of Id2 is the result of increased E protein activity.

The E-box binding bHLH transcription factor Ascl2 has been shown to drive robust T_{FH} differentiation by inducing CXCR5 when overexpressed in CD4$^+$ T cells[22]. E proteins *Tcf3* and *Tcf12* (HEB) are both highly expressed in T_{FH} cells early after LCMV infection (Supplementary Fig. 5b)[26]. In contrast, *Ascl2* is essentially undetectable in either T_{FH} or T_H1 cells at the same time point (Supplementary Fig. 5b). Retroviruses overexpressing the *Tcf3* isoforms E12, E47 or Ascl2 all induced CXCR5 expression by CD4$^+$ T cells *in vitro* (Fig. 5b). Ectopic expression of E47 led to enhanced expression of CXCR5 by both early T_H1 cells and early T_{FH} cells when compared to their GFP-RV$^+$ counterparts *in vivo* (Fig. 5c, Supplementary Fig. 5c).

Given that Id2 inhibits the transcriptional activity of E proteins and E proteins induce CXCR5 expression, we investigated whether Id2 inhibited T_{FH} differentiation by preventing expression of CXCR5. *Id2*-RV$^+$ or GFP-RV$^+$ NIP CD4$^+$ T cells were transferred into B6 mice, which were infected with LCMV. *Id2*-RV$^+$ NIP CD4$^+$ T cells displayed decreased differentiation into early T_{FH} cells (Fig. 5d,f,g) and impaired CXCR5 expression (Fig. 5e, Supplementary Fig. 5e). Overexpression of *Id2* did not impact expression of T-bet or accumulation of *Id2*-RV$^+$ NIP CD4$^+$ T cells (Supplementary Fig. 5d,f). Similar to what was previously observed, *Id2*-RV$^+$ NIP CD4$^+$ T cells poorly differentiated into T_{FH} cells 6 days

after LCMV infection (Fig. 5h,j,k, Supplementary Fig. 5g–j), with impaired CXCR5 expression by T_{FH} cells (Fig. 5i, Supplementary Fig. 5k). Additionally, accumulation of *Id2*-RV^+ GC T_{FH} cells was impaired (Fig. 5h,j,k). Next, we constitutively co-expressed E proteins, Ascl2 and Id2 in $CD4^+$ T cells. E proteins were expressed from a GFP reporter RV while Id2 was expressed from an Ametrine reporter RV. As expected, the E proteins E12, E47 and Ascl2 drove strong CXCR5 expression when $CD4^+$ T cells were co-transduced with an empty Ametrine-RV (Fig. 5l). When Id2-Ame-RV was introduced into E12- or E47-RV^+ $CD4^+$ T cells, there was a reduction in CXCR5 expression (Fig 5l) by $GFP^+Ametrine^+$ cells. Surprisingly, Id2 was not able to block the Ascl2-driven induction of CXCR5 (Fig. 5l). These data indicate that Id2 prevents E proteins from inducing CXCR5 expression.

Bcl6 inhibits *Id2* expression

Our data show that the Id2-E protein axis modulates T_H1 and T_{FH} differentiation, and that Id2 inhibits expression of *Cxcr5*. The transcriptional repressor Bcl6 is essential for T_{FH} differentiation and is important for CXCR5 expression by T_{FH} cells *in vivo*[8,25,36], but it does not directly regulate *Cxcr5*[22,37]. We therefore asked whether Bcl6 induces CXCR5 expression by inhibiting *Id2* transcription. Bcl6 ChIP-Seq of primary tonsillar GC T_{FH} revealed recruitment of BCL6 to the *ID2* locus (Fig. 6a)[37], which was confirmed by ChIP-qPCR (Fig. 6b). To test whether Bcl6 represses *Id2* expression, we transduced *Bcl6*$^{fl/fl}$ CD4-Cre^+ SMARTA $CD4^+$ T cells (*Bcl6*$^{-/-}$) with GFP-RV or Bcl6-RV, transferred RV^+ cells into B6 mice, infected with LCMV, and assessed expression of *Id2* (Supplementary Fig. 6a, Fig. 6c). Re-introduction of Bcl6 into *Bcl6*$^{-/-}$ cells led to significant repression of *Id2* in IL-2Rα^{hi} Th1 cells (Fig. 6c). Recent work demonstrated that separate domains of Bcl6 control T_{FH} differentiation, and mutation of lysine K379Q significantly hinders the activity of Bcl6[27,35]. Introduction of the Bcl6 K379Q mutant into *Bcl6*$^{-/-}$ cells failed to repress *Id2* compared to WT Bcl6 (Fig. 6c). Thus, Bcl6 directly represses *Id2* in $CD4^+$ T cells.

We also asked how *Bcl6* gene copy number affected *Id2* expression. *Bcl6*$^{-/-}$, *Bcl6*$^{+/-}$ or WT CD4-Cre^+ SMARTA $CD4^+$ T cells were transferred into B6 mice and IL-2Rα^{hi} (T_H1) and IL-2Rα^{lo} (T_{FH}) cells were sorted following LCMV infection (Supplementary Fig. 6b). As expected, WT T_{FH} cells had reduced expression of *Id2* compared to T_H1 cells (Fig. 6d). *Id2* expression was significantly increased in IL-2Rα^{lo} Bcl6$^{+/-}$ cells in comparison to WT cells (Fig. 6d). Further, complete loss of *Bcl6* resulted in a significant upregulation of *Id2* expression in IL-2Rα^{lo} cells compared to IL-2Rα^{lo} Bcl6$^{+/-}$ and WT cells (Fig. 6d). Thus, Bcl6 inhibits *Id2* and *Bcl6* haploinsufficiency results in inappropriate Id2 expression.

Discussion

E and Id proteins are pivotal regulators of lymphocyte development and function. Here, we investigated an unexplored role for Id2 in the differentiation T_H cells in response to acute viral infection and show that Id2 controls the balance of T_H1/T_{FH} by inhibiting E protein activity. Id2 and Id3 are preferentially expressed in T_H1 and T_{FH} cells, respectively. Reduction of Id2 levels in $CD4^+$ T cells results in a higher proportion of T_{FH} cells. Complete ablation of Id2 hampered T_H1 generation, resulting in an abnormal effector population exhibiting mixed traits of T_H1 and T_{FH} lineages. Further, Bcl6 specifically inhibits *Id2* to

ensure E protein activity, driving a portion of the T_{FH} program, thus establishing Id2 as a critical enforcer of proper T_H differentiation.

Reduction of Id2 levels shifts the balance of T_H1/T_{FH} cells indicating that partial expression of Id2 can inhibit enough E protein expression to maintain both helper populations while still biasing cells towards the T_{FH} lineage. Strikingly, $CD4^+$ T cells that completely lack *Id2* lose the ability to form a T_H1 effector cell population, while maintaining an intact T_{FH} population. *Id2*-deficient effector cells exhibit weak expression of T_H1-associated genes and show simultaneous upregulation of a large portion of the T_{FH} gene program (*Cxcr5*, *Il6ra*, *Lef1* and *Tcf7*, but not *Bcl6*, *Icos* and *Pdcd1*). *Id2*-deficient cells may be unable to commit to one lineage for a number of reasons. While they adopt aspects of the T_{FH} transcriptional program, *Id2*-deficient cells also upregulate and maintain high levels of *Id3*, *Foxo1* and *Il2ra*, which may explain this dichotomy. Foxo1 specifically inhibits T_{FH} development[38,39]. Within the first two cell divisions, expression of IL-2Rα is a key factor in driving the T_H1 lineage decision[25]. Their expression in the absence of Id2 may counterbalance the T_{FH} gene program. Thus, Id2 and E proteins are powerful regulators of key T_{FH}-associated genes and many T_H1-associated genes, but the unusual phenotype of *Id2*-deficient effector $CD4^+$ T cells demonstrates that Id2 and E proteins control gene sets that do not *per se* result in polarized differentiation of T_H1 and T_{FH} cells.

Previous work demonstrated a role for Id3 in regulating the T_{FH} gene expression program[20,22,24,40]. Our work further shows that specific deletion of Id3 in T_H cells promotes T_{FH}/GC T_{FH} formation but does not impact T_H1 differentiation following infection. Both differential expression patterns and unique binding partners are plausible explanations as to how Id2 and Id3 may control distinct T_H subsets. They may inhibit DNA binding of different E proteins with differing affinities and have differentially regulated binding activity and protein stability. In support of this, we observe that Id2 inhibits E47 but not Ascl2 induction of *Cxcr5*. Loss of Id2 dramatically impairs T_H1 differentiation, but Id3-deficiency does not phenocopy Id2-deficiency, instead enhancing T_{FH} and GC T_{FH} differentiation. These observations support the hypothesis that inhibition of E proteins alters the T_H1/T_{FH} balance: Id2 is important in the upregulation of T_H1 genes while Id3 restrains T_{FH} differentiation.

Ascl2 has been suggested to act upstream of Bcl6 to regulate early T_{FH} differentiation[22]. However, Ascl2 is generally not detectable in naive $CD4^+$ T cells[41–43](Immgen.org), nor early T_{FH} cells[26]. Instead, Ascl2 expression is reported for fully differentiated GC T_{FH} cells in mice and humans[22,43]. The high expression of E2A and HEB early after LCMV infection suggests that these E proteins, not Ascl2, direct early T_{FH} differentiation. Interestingly, Ascl2-induced expression of CXCR5 was not dampened by co-expression of Id2. GC T_{FH} have the highest levels of CXCR5 expression and Ascl2 may be important for amplifying expression at later stages of T_{FH} differentiation into GC T_{FH} cells.

There are multiple plausible models for the coordination of genes regulating the earliest stages of T_{FH} differentiation *in vivo*. Bcl6 function is critical for T_{FH} differentiation[2,27,35], and can be detected as early as the second cell division *in vivo*[25]. *Tcf7* and *Lef1*, both of which are known E protein targets[44], are epistatic to Bcl6 and promote T_{FH} differentiation by enhancing expression of Bcl6, IL-6R and ICOS and repressing *Prdm1*[26,45,46]. Notably,

we observed increased expression of *Tcf7*, *Lef1*, and *Il6ra* in the absence of Id2, supporting the idea that E proteins such as E2A and HEB normally promote TCF-1 and LEF-1 expression. In this regard, Id2 and E proteins act upstream of Bcl6. However, our data also demonstrate that Bcl6 directly represses *Id2* expression. Altogether these data suggest that positive feedback mechanisms involving TCF-1, LEF-1, Bcl6, IL-6R, ICOS, and E proteins support T_{FH} differentiation under low Id2 conditions, and that a feedforward loop can potentially be generated by starting at any of several genes in that gene network.

The relationship between E/Id proteins, Bcl6 and CXCR5 expression is of particular interest. Ectopic expression of Bcl6 in human $CD4^+$ T cells results in CXCR5 expression[47]. Coordinated expression of Bcl6 and CXCR5 in early T_{FH} cells is observed in multiple *in vivo* models[25,36,48,49]. Yet Bcl6 does not bind to *Cxcr5*[37], and thus must regulate its expression indirectly. One mechanism involves repression of *Cxcr5* by Blimp-1[7]. But naive T cells do not express Blimp-1, indicating that this mechanism primarily regulates later CXCR5 expression. Here, we provide a new mechanism whereby Bcl6 inhibits *Id2* expression, which yields enhanced E protein activity to drive *Cxcr5* expression.

Our data uniquely position Id2, Bcl6 and E proteins in a regulatory triad that controls the balance of T_H1 and T_{FH} differentiation. Through inhibition of E proteins, high expression of Id2 in the T_H1 population enforces proper development of the T_H1 lineage. Early expression of Bcl6 in T_{FH} cells ensures repression of Id2, allowing E proteins to drive T_{FH} differentiation. Thus, dichotomous expression of Id2 is critical in ensuring the reciprocal development of T_H1 and T_{FH} cell differentiation.

ONLINE METHODS

Mice

$CD4\text{-}Cre^+$ mice were from Jackson Laboratory. Mouse strains described below were bred and housed in specific pathogen–free conditions in accordance with the Institutional Animal Care and Use Guidelines of the University of California San Diego or the La Jolla Institute. Id2-YFP[14], Id3-GFP[24], $Id2^{fl/fl}$[28], $Id3^{fl/fl}$[34], SMARTA TCR transgenic (specific for LCMV gp66-77)[50], $Bcl6^{fl/fl}$[51] CD45.1 congenic, NIP TCR transgenic (specific for LCMV NP311-325)[35] and OT-II TCR transgenic (specific for OVA 323-339) mice were on a fully B6 background. Recipient C57BL/6J mice were either bred at UCSD or received from The Jackson Laboratory. Both male and female mice were used throughout the study, with sex and age matched T cell donors and recipients.

LCMV Infection and protein immunizations

Recipient mice were infected by intraperitoneal injection of 2×10^5 or 5×10^5 plaque-forming units of LCMV-Armstrong for days 6/7 or 3 analysis, respectively. In adoptive transfer experiments of naive $CD4^+$ T cells, LCMV infection was performed one day after cell transfer. A total of 20 μg of 4-Hydroxy-3-nitrophenylacetyl-OVA (NP_{16}-OVA; Biosearch Technologies) was prepared in 5% alum (Aluminum potassium sulfate, Sigma) in a total volume of 20 μL and injected into each footpad.

Toxoplasma gondii infection and lymphocyte isolation from small intestine

The ME49 strain of *T. gondii* was maintained in CBA/CaJ mice by intraperitoneal injection of 20 cysts and cysts were obtained from brain homogenates after 5–6 weeks. Mice were infected with 40 cysts of ME49 by gavage. Small intestine was harvested on day 7-post infection to analyze T_H1 response. To isolate lamina propria lymphocytes, small intestine were cut and washed with plain RPMI-1640, and epithelial cells were removed by incubation with 5 mM EDTA and 1mM DTT for 20 min at 37 °C, followed by enzyme digestion with 0.16 U/ml liberase TL (Roche) for 30 min at 37 °C. Lymphocytes were enriched by centrifugation with 47% percoll.

Flow cytometry and histology

Single-cell suspensions of spleen or draining popliteal lymph nodes were prepared by standard gentle mechanical disruption. Surface staining for flow cytometry was done with monoclonal antibodies against CD4 (RM4-5, 1:400), CD8 (53-6.7, 1:400), CD45.1 (A20, 1:400), CD25 (PC61.5, 1:400), B220 (RA3-6B2, 1:400), IgD (11-26, 1:400), PD-1 (J43, 1:400) and CD138 (eBiosciences, 1:500); PSGL-1 (2PH1, 1:800), CD138 (281-2, 1:500), Fas (Jo2, 1:400) (from BD Biosciences); SLAM (TC15-12F12.2, 1:400), CD25 (PC61, 1:400), CD4 (GK1.5, 1:400), Ly6C (AK1.4, 1:800) (BioLegend) and PNA (Vector Laboratories). Stains were done for 30 min at 4 °C in PBS supplemented with 0.5% bovine serum albumin and 0.1% sodium azide, unless specified otherwise. PE-labeled IA^b/GP66–77 tetramer was supplied by the National Institute of Health (NIH) tetramer core facility. Single-cell suspensions were stained with tetramer at 37 °C for 2 h. CXCR5 staining was done as described[52], using purified anti-CXCR5 (2G8; BD Pharmingen) for 1 h, followed by biotinylated anti-rat IgG (Jackson Immunoresearch), and then by PE-, PE-Cy7- or APC-labeled streptavidin (eBioscience) at 4 °C in PBS supplemented with 0.5% bovine serum albumin, 2% fetal calf serum, and 2% normal mouse serum. Intracellular staining was performed with an Alexa 647- or PE-conjugated monoclonal antibody to Bcl6 (clone K112-91; BD Pharmingen, 1:20), TCF1 (clone C63D9; Cell Signaling, 1:200), IFN-γ (clone XMG1.2; eBioscience, 1:200), T-bet (clone 4B10; eBioscience, 1:200), FoxP3 (clone FJK-16s; eBioscience, 1:200) and the Foxp3 ICS kit buffers and protocol (eBioscience). Stained cells were analyzed using LSRII, LSRFortessa or LSRFortessa X-20 (BD) and FlowJo software (TreeStar). All sorting was done on a FACS Aria (BD Biosciences). For RT-PCR analyses, early T_H1 (IL-2Rα$^+$) and T_{FH} (IL-2Rα$^-$) amongst total or RV$^+$ SMARTA CD4$^+$ T cells were sorted 3 days after infection with LCMV. Histology was performed as previously described[53].

ELISA

Nunc MaxiSorp plates (Thermo Fisher Scientific) were coated overnight at 4 °C with 1 μg/mL NP_{23}-BSA (Biosearch Technologies) or with a 1:60 dilution of LCMV lysate (prepared from LCMV-infected BHK cells) in PBS. Plates were blocked with PBS + 0.2% Tween-20 + 1% BSA for 90 min at 25°C. After washing, mouse serum was added in a dilution series in PBS + 0.2% Tween-20 + 1% BSA and incubated for 90 min. After washing, horseradish peroxidase (HRP)-conjugated goat anti-mouse IgG (Thermo Fisher Scientific) was added at 1:5,000 in PBS + 0.2% Tween-20 + 1% BSA for 90 min at 25°C.

Colorimetric detection was performed using a TMB substrate kit (Thermo Fisher Scientific). Color development was stopped after approximately 10 min with 2 N H_2SO_4, and absorption was measured at 450 nm.

Retroviral vectors, transductions and cell transfers

shRNAmir and pMIG, Bcl6 MIG and middle domain mutant Bcl6 (K379Q) vectors were described previously[27,52]. E12, E47, Ascl2, Id2 and Id3 were cloned into the pMIG or pMIA vectors, which contain an IRES-GFP or IRES-mAmetrine, respectively. Virions were produced by transfection of the PLAT-E cell line, as described previously[8]. Culture supernatants were collected 24 and 48 h after transfection, filtered through a 0.45 μm syringe filter and stored at 4°C until transduction. $CD4^+$ T cells were isolated from whole splenocytes by negative selection (Stemcell Technologies) and resuspended in D-10 (DMEM + 10% fetal calf serum, supplemented with 2 mM Glutamax (Gibco) and 100 U/mL Penicillin/Streptomycin (Gibco)) with 2 ng/mL recombinant human IL-7 (Peprotech) and 50 μM β-mercaptoethanol (BME). 2×10^6 cells were stimulated in 24-well plates pre-coated with 8 μg/mL anti-CD3 (17A2; BioXcell) and anti-CD28 (37.51; BioXcell). At 24 and 36 h after stimulation, cells were transduced by adding RV supernatants supplemented with 50 μM BME and 8 μg/mL polybrene (Millipore), followed by centrifugation for 90 min at 524 x *g* at 37 °C. Following each transduction, the RV-containing medium was replaced with D-10 + 50 μM BME + 10 ng/mL human IL-2. After 72 h of *in vitro* stimulation, $CD4^+$ T cells were transferred into six-well plates in D-10 + 50 μM BME + 10 ng/mL human IL-2, followed by incubation for 2.5 days. One day before transfer, the culture medium was replaced with D-10 + 50 μM BME + 2 ng/mL human IL-7. Transduced cells were sorted based on reporter expression (FACSAria; BD Biosciences). Transfer of sorted cells into recipient mice was performed by intravenous injection via the retro-orbital sinus. Transferred cells were allowed to rest in host mice for 3-4 days before infection or immunization. 2×10^4 or 4×10^5 transduced $CD4^+$ T cells were transferred into each mouse for day 6 or 3 analysis, respectively. For protein immunization, 1×10^5 transduced $CD4^+$ T cells were transferred into each mouse. (Fig. 5a) DNA fragments encoding shRNAs targeting mouse *Tcf3* or *Cd8a* were subcloned into a custom retroviral vector containing the miR30 backbone plus the murine PGK promoter and dsRED as a reporter. 1×10^6 naive $Id2^{+/+}$CD4-Cre^+ and $Id2^{fl/fl}$CD4-Cre^+ SMARTA $CD4^+$ T cells were stimulated in 24-well plates pre-coated with anti-CD3 and anti-CD28 for 18 h. Following stimulation, cells were transduced by adding RV supernatants supplemented with 100 U/ml human IL-2 and 8 μg/mL polybrene, followed by centrifugation for 90 min at 2000 × *g* at 37 °C. Following transduction, cells were incubated for 3 h at 37 °C. 5×10^4 cells were transferred into day −1 LCMV infected hosts and remaining cells were cultured *in vitro* with D-10 + 50 U/mL human IL-2 in a parallel time course to assess for knockdown efficiency.

Microarray and ChIP-seq

$Id2^{+/+}$ CD4-Cre^+ and $Id2^{fl/fl}$ CD4-Cre^+ $CD4^+$ T cells (pooled from 5 mice) were isolated via flow cytometry on day 7 of LCMV infection (FacsARIA, BD). For microarray analysis, RNA was extracted with TRIzol reagent, amplified and hybridized to the Affymetrix Mouse Gene 1.0 ST Array. Data were normalized and analyzed with the GenePattern software suite.

E2A Bio-Chip was performed as previously described on total thymocytes from *Tcfe2a*$^{Bio/Bio}$ *Rosa26*$^{BirA/BirA}$ mice[16,54].

Quantitative RT-PCR and ChIP-qPCR

Total RNA from the sorted cells was extracted and reverse-transcribed, and quantitative PCR was performed using SYBR Select MasterMix (Thermo Fisher Scientific). Results were normalized to the expression of *Gapdh* transcripts. Primary GC T_{FH} were isolated from human tonsil by staining with biotin-conjugated PD-1 (J105, eBioscience) followed by isolation using Streptavidin microbeads (Miltenyi). GC T_{FH} were crosslinked with 1% formaldehyde and then quenched with 125 mM glycine. Cells were lysed in RIPA buffer (150 mM NaCl, 1% NP-40, 0.5% Na-Deoxycholate, 0.1% SDS, 50 mM Tris and 5 mM EDTA) supplemented with protease inhibitors (Thermo Fisher Scientific) and 0.5 mM PMSF followed by sonication and isolation of chromatin. Protein G Dynabeads (Life Technologies) were conjugated to antibodies specific to Bcl6 (N-3 and C-19, Santa Cruz). Normal rabbit IgG (Santa Cruz) was used as a control. Chromatin was immunoprecipitated using the conjugated beads, eluted, and reverse crosslinked using 0.3 M NaCl at 65 °C overnight. qPCR was performed on isolated DNA and sample values were given as a percentage of input. Primers are listed in Supplementary Fig. 6c.

Statistical Methods

Statistical tests were performed using Prism 6.0 (GraphPad). Significance was determined by unpaired Student's *t*-test with a 95% confidence interval.

Supplementary Material

Refer to Web version on PubMed Central for supplementary material.

Acknowledgments

We would like to thank the members of the Goldrath and Crotty Labs for thoughtful discussion, Bingfei Yu for assistance with bioinformatics analysis and Ivan Bilic and Meinrad Busslinger for providing E2A Bio-ChiP-seq data. Supported by the National Institutes of Health (1F31AG043222-01A1 to L.A.S., AI108651 to L-F.L., AI067545 to A.W.G., AI109976 to A.W.G. and S.C.), the Fonds de la recherche Québec - Santé (Postdoctoral Training Award to S.B.), The Damon Runyon Cancer Research Foundation (Fraternal Order of Eagles Fellowship DRG-2069-11 to J.P.S-B.) and the Leukemia and Lymphoma Society (to K.D.O and A.W.G.).

References

1. Zhu J, Yamane H, Paul WE. Differentiation of effector CD4 T cell populations (*). Annual review of immunology. 2010; 28:445–489.
2. Crotty S. T follicular helper cell differentiation, function, and roles in disease. Immunity. 2014; 41:529–542. [PubMed: 25367570]
3. Vahedi G, et al. Helper T-cell identity and evolution of differential transcriptomes and epigenomes. Immunological reviews. 2013; 252:24–40. [PubMed: 23405893]
4. Nurieva RI, et al. Bcl6 mediates the development of T follicular helper cells. Science. 2009; 325:1001–1005. [PubMed: 19628815]
5. Yu D, et al. The transcriptional repressor Bcl-6 directs T follicular helper cell lineage commitment. Immunity. 2009; 31:457–468. [PubMed: 19631565]
6. Nakayamada S, et al. Early Th1 cell differentiation is marked by a Tfh cell-like transition. Immunity. 2011; 35:919–931. [PubMed: 22195747]

7. Oestreich KJ, Mohn SE, Weinmann AS. Molecular mechanisms that control the expression and activity of Bcl-6 in TH1 cells to regulate flexibility with a TFH-like gene profile. Nature immunology. 2012; 13:405–411. [PubMed: 22406686]
8. Johnston RJ, et al. Bcl6 and Blimp-1 are reciprocal and antagonistic regulators of T follicular helper cell differentiation. Science. 2009; 325:1006–1010. [PubMed: 19608860]
9. Cannarile MA, et al. Transcriptional regulator Id2 mediates CD8+ T cell immunity. Nature immunology. 2006; 7:1317–1325. [PubMed: 17086188]
10. de Pooter RF, Kee BL. E proteins and the regulation of early lymphocyte development. Immunological reviews. 2010; 238:93–109. [PubMed: 20969587]
11. D'Cruz LM, Stradner MH, Yang CY, Goldrath AW. E and Id proteins influence invariant NKT cell sublineage differentiation and proliferation. Journal of immunology. 2014; 192:2227–2236.
12. Jones-Mason ME, et al. E protein transcription factors are required for the development of CD4(+) lineage T cells. Immunity. 2012; 36:348–361. [PubMed: 22425249]
13. Eberl G, Colonna M, Di Santo JP, McKenzie AN. Innate lymphoid cells. Innate lymphoid cells: a new paradigm in immunology. Science. 2015; 348:aaa6566. [PubMed: 25999512]
14. Yang CY, et al. The transcriptional regulators Id2 and Id3 control the formation of distinct memory CD8+ T cell subsets. Nature immunology. 2011; 12:1221–1229. [PubMed: 22057289]
15. D'Cruz LM, Lind KC, Wu BB, Fujimoto JK, Goldrath AW. Loss of E protein transcription factors E2A and HEB delays memory-precursor formation during the CD8+ T-cell immune response. European journal of immunology. 2012; 42:2031–2041. [PubMed: 22585759]
16. Masson F, et al. Id2-mediated inhibition of E2A represses memory CD8+ T cell differentiation. Journal of immunology. 2013; 190:4585–4594.
17. Ji Y, et al. Repression of the DNA-binding inhibitor Id3 by Blimp-1 limits the formation of memory CD8+ T cells. Nature immunology. 2011; 12:1230–1237. [PubMed: 22057288]
18. Gao P, et al. Dynamic changes in E-protein activity regulate T reg cell development. The Journal of experimental medicine. 2014; 211:2651–2668. [PubMed: 25488982]
19. Maruyama T, et al. Control of the differentiation of regulatory T cells and T(H)17 cells by the DNA-binding inhibitor Id3. Nature immunology. 2011; 12:86–95. [PubMed: 21131965]
20. Miyazaki M, et al. Id2 and Id3 maintain the regulatory T cell pool to suppress inflammatory disease. Nature immunology. 2014; 15:767–776. [PubMed: 24973820]
21. Lin YY, et al. Transcriptional regulator Id2 is required for the CD4 T cell immune response in the development of experimental autoimmune encephalomyelitis. Journal of immunology. 2012; 189:1400–1405.
22. Liu X, et al. Transcription factor achaete-scute homologue 2 initiates follicular T-helper-cell development. Nature. 2014; 507:513–518. [PubMed: 24463518]
23. Choi YS, et al. Bcl6 expressing follicular helper CD4 T cells are fate committed early and have the capacity to form memory. Journal of immunology. 2013; 190:4014–4026.
24. Miyazaki M, et al. The opposing roles of the transcription factor E2A and its antagonist Id3 that orchestrate and enforce the naive fate of T cells. Nature immunology. 2011; 12:992–1001. [PubMed: 21857655]
25. Choi YS, et al. ICOS receptor instructs T follicular helper cell versus effector cell differentiation via induction of the transcriptional repressor Bcl6. Immunity. 2011; 34:932–946. [PubMed: 21636296]
26. Choi YS, et al. LEF-1 and TCF-1 orchestrate TFH differentiation by regulating differentiation circuits upstream of the transcriptional repressor Bcl6. Nature immunology. 2015; 16:980–990. [PubMed: 26214741]
27. Nance, JP., et al. Bcl6 middle domain repressor function is required for T follicular helper cell differentiation and utilizes the corepressor MTA3. Proceedings of the National Academy of Sciences of the United States of America; 2015;
28. Niola F, et al. Id proteins synchronize stemness and anchorage to the niche of neural stem cells. Nature cell biology. 2012; 14:477–487. [PubMed: 22522171]

29. Johnston RJ, Choi YS, Diamond JA, Yang JA, Crotty S. STAT5 is a potent negative regulator of TFH cell differentiation. The Journal of experimental medicine. 2012; 209:243–250. [PubMed: 22271576]
30. Poholek AC, et al. In vivo regulation of Bcl6 and T follicular helper cell development. Journal of immunology. 2010; 185:313–326.
31. Ray JP, et al. The Interleukin-2-mTORc1 Kinase Axis Defines the Signaling, Differentiation, and Metabolism of T Helper 1 and Follicular B Helper T Cells. Immunity. 2015; 43:690–702. [PubMed: 26410627]
32. Amir el AD, et al. viSNE enables visualization of high dimensional single-cell data and reveals phenotypic heterogeneity of leukemia. Nature biotechnology. 2013; 31:545–552.
33. Sher A, et al. Induction and regulation of IL-12-dependent host resistance to Toxoplasma gondii. Immunol Res. 2003; 27:521–528. [PubMed: 12857995]
34. Guo Z, et al. Modeling Sjogren's syndrome with Id3 conditional knockout mice. Immunol Lett. 2011; 135:34–42. [PubMed: 20932862]
35. Nance JP, Belanger S, Johnston RJ, Takemori T, Crotty S. Cutting Edge: T Follicular Helper Cell Differentiation Is Defective in the Absence of Bcl6 BTB Repressor Domain Function. Journal of immunology. 2015; 194:5599–5603.
36. Pepper M, Pagan AJ, Igyarto BZ, Taylor JJ, Jenkins MK. Opposing signals from the Bcl6 transcription factor and the interleukin-2 receptor generate T helper 1 central and effector memory cells. Immunity. 2011; 35:583–595. [PubMed: 22018468]
37. Hatzi K, et al. BCL6 orchestrates Tfh cell differentiation via multiple distinct mechanisms. The Journal of experimental medicine. 2015; 212:539–553. [PubMed: 25824819]
38. Xiao R, et al. Identification and characterization of a cathepsin D homologue from lampreys (Lampetra japonica). Developmental and comparative immunology. 2015; 49:149–156. [PubMed: 25450905]
39. Stone EL, et al. ICOS coreceptor signaling inactivates the transcription factor FOXO1 to promote Tfh cell differentiation. Immunity. 2015; 42:239–251. [PubMed: 25692700]
40. Miyazaki M, et al. The E-Id protein axis modulates the activities of the PI3K-AKT-mTORC1-Hif1a and c-myc/p19Arf pathways to suppress innate variant TFH cell development, thymocyte expansion, and lymphomagenesis. Genes & development. 2015; 29:409–425. [PubMed: 25691468]
41. Kitano M, et al. Bcl6 protein expression shapes pre-germinal center B cell dynamics and follicular helper T cell heterogeneity. Immunity. 2011; 34:961–972. [PubMed: 21636294]
42. Hale JS, et al. Distinct memory CD4+ T cells with commitment to T follicular helper- and T helper 1-cell lineages are generated after acute viral infection. Immunity. 2013; 38:805–817. [PubMed: 23583644]
43. Yusuf I, et al. Germinal center T follicular helper cell IL-4 production is dependent on signaling lymphocytic activation molecule receptor (CD150). Journal of immunology. 2010; 185:190–202.
44. Lin YC, et al. A global network of transcription factors, involving E2A, EBF1 and Foxo1, that orchestrates B cell fate. Nature immunology. 2010; 11:635–643. [PubMed: 20543837]
45. Wu T, et al. TCF1 Is Required for the T Follicular Helper Cell Response to Viral Infection. Cell reports. 2015; 12:2099–2110. [PubMed: 26365183]
46. Xu L, et al. The transcription factor TCF-1 initiates the differentiation of TFH cells during acute viral infection. Nature immunology. 2015; 16:991–999. [PubMed: 26214740]
47. Kroenke MA, et al. Bcl6 and Maf cooperate to instruct human follicular helper CD4 T cell differentiation. Journal of immunology. 2012; 188:3734–3744.
48. Choi YS, Eto D, Yang JA, Lao C, Crotty S. Cutting edge: STAT1 is required for IL-6-mediated Bcl6 induction for early follicular helper cell differentiation. Journal of immunology. 2013; 190:3049–3053.
49. Baumjohann D, Okada T, Ansel KM. Cutting Edge: Distinct waves of BCL6 expression during T follicular helper cell development. Journal of immunology. 2011; 187:2089–2092.
50. Oxenius A, Bachmann MF, Zinkernagel RM, Hengartner H. Virus-specific MHC-class II-restricted TCR-transgenic mice: effects on humoral and cellular immune responses after viral infection. European journal of immunology. 1998; 28:390–400. [PubMed: 9485218]

51. Kaji T, et al. Distinct cellular pathways select germline-encoded and somatically mutated antibodies into immunological memory. The Journal of experimental medicine. 2012; 209:2079–2097. [PubMed: 23027924]

52. Chen R, et al. In vivo RNA interference screens identify regulators of antiviral CD4(+) and CD8(+) T cell differentiation. Immunity. 2014; 41:325–338. [PubMed: 25148027]

53. Doedens AL, et al. Hypoxia-inducible factors enhance the effector responses of CD8(+) T cells to persistent antigen. Nature immunology. 2013; 14:1173–1182. [PubMed: 24076634]

54. Ebert A, et al. The distal V(H) gene cluster of the Igh locus contains distinct regulatory elements with Pax5 transcription factor-dependent activity in pro-B cells. Immunity. 2011; 34:175–187. [PubMed: 21349430]

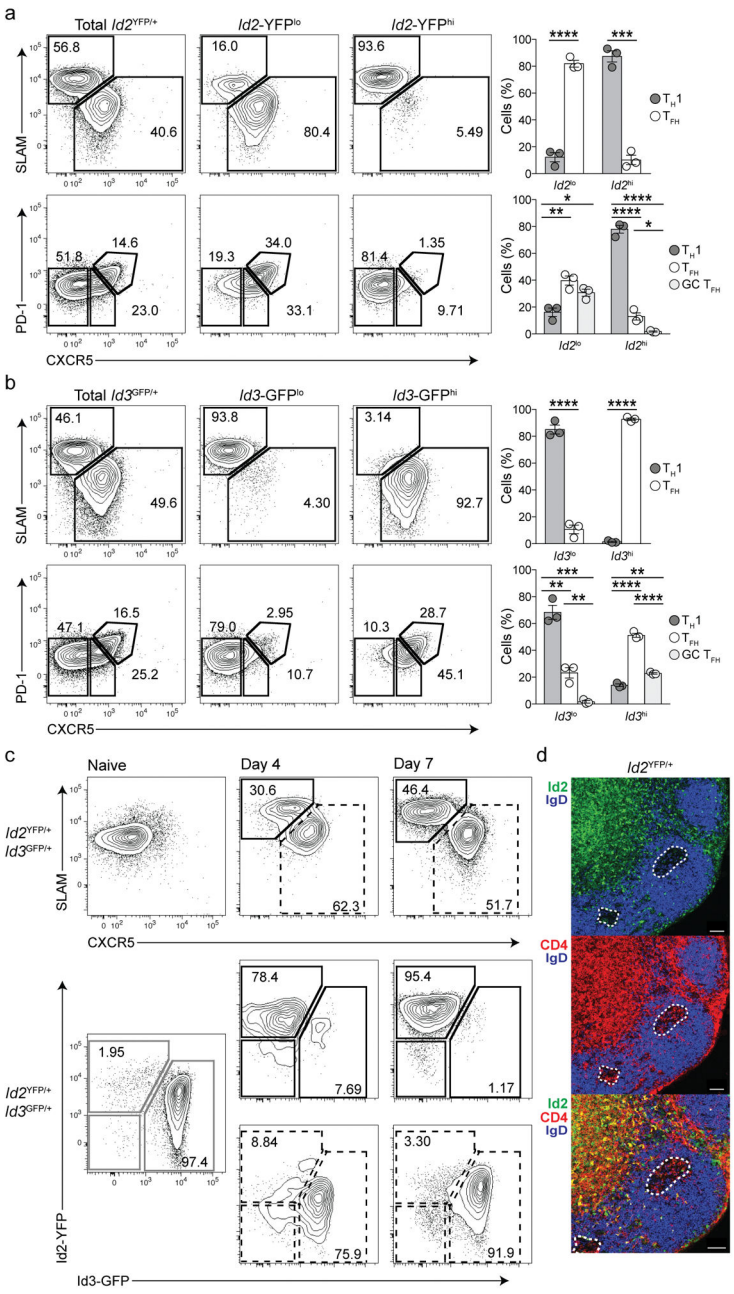

Figure 1. Differential Id2 and Id3 expression defines T_H1 and T_{FH} cell subsets

Id2$^{YFP/+}$ (**a**) or *Id3*$^{GFP/+}$ (**b**) SMARTA CD4$^+$ T cells were transferred into B6 mice and analyzed 7 days after LCMV infection. T_H1 (SLAM$^+$CXCR5$^-$ or CXCR5$^-$PD-1$^-$), T_{FH} (SLAM^{lo}CXCR5$^+$ or CXCR5$^+$PD-1$^-$) or GC T_{FH} (CXCR5$^+$PD-1$^+$) cell development in the indicated SMARTA CD4$^+$ T cell populations was analyzed by flow cytometry and quantified. (**c**) *Id2*$^{YFP/+}$*Id3*$^{GFP/+}$ SMARTA CD4$^+$ T cells were transferred into B6 mice and analyzed 0, 4 or 7 days after LCMV infection. Flow cytometric analysis of Id2-YFP and Id3-GFP expression (bottom plots) in SLAM$^+$CXCR5$^-$ (black lines) or CXCR5$^+$SLAM^{lo} (dashed lines) populations (top plots). (**d**) *Id2*$^{YFP/+}$ reporter mice were immunized

subcutaneously with phycoerythrin (PE) emulsified in TiterMax Gold Adjuvant and analyzed by histology 13 days later. Draining lymph node sections were stained with IgD (blue) and CD4 (red). Id2-YFP reporter expression is shown in green. *p<0.05, **p<0.01, ***p<0.001, ****p<0.0001 (two-tailed unpaired Student's *t* test). Data are representative of three experiments (**a–c**), each with n = 3 mice per group, or are representative of two experiments (**d**), each with n = 2 mice per group (mean ± s.e.m.).

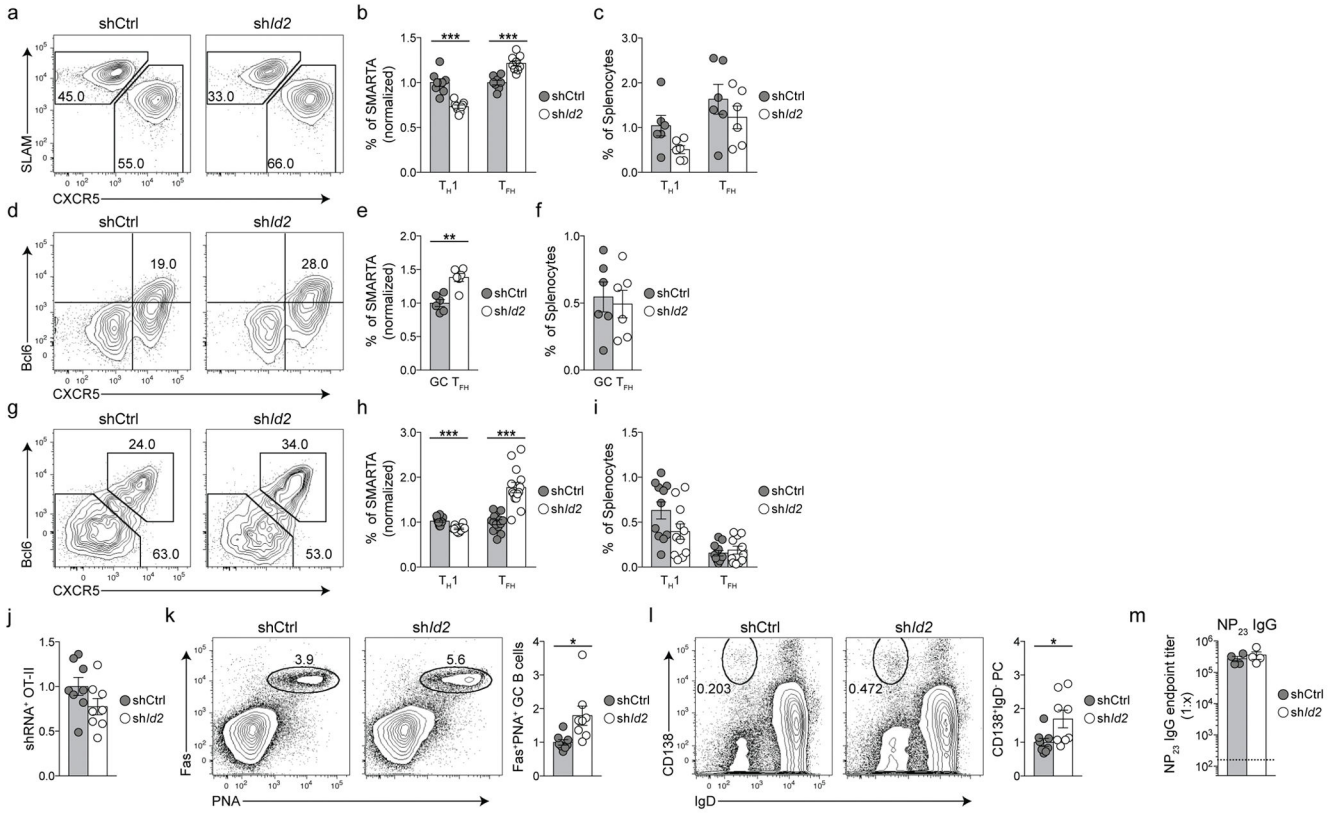

Figure 2. Id2 knockdown results in increased T_{FH} differentiation

SMARTA $CD4^+$ T cells transduced with the indicated shRNAmir-RV were transferred into B6 mice and analyzed 6 (**a–f**) or 3 days (**g–i**) after LCMV infection. (**a–c**) T_{FH} ($CXCR5^+SLAM^{lo}$) and T_H1 ($SLAM^+CXCR5^-$) differentiation was analyzed by flow cytometry (**a**) and quantified as a fraction of SMARTA $CD4^+$ T cells (**b**) or total splenocytes (**c**). (**d–f**) GC T_{FH} ($CXCR5^+Bcl6^+$) differentiation was analyzed by flow cytometry (**d**) and quantified as a fraction of SMARTA $CD4^+$ T cells (**e**) or total splenocytes (**f**). (**g–i**) T_{FH} ($CXCR5^+Bcl6^+$) and T_H1 ($CXCR5^-Bcl6^-$) cell development was analyzed by flow cytometry (**g**) and quantified as a fraction of SMARTA $CD4^+$ T cells (**h**) or total splenocytes (**i**). (**j–m**) OT-II $CD4^+$ T cells transduced with the indicated shRNAmir-RV were transferred into *Bcl6*$^{fl/fl}$ CD4-Cre^+ mice and analyzed 11 days after footpad immunization with NP-OVA in alum. (**j**) Quantitation of OT-II $CD4^+$ T cells. GC B cells (Fas^+PNA^+) (**k**) and plasma cells ($CD138^+IgD^-$) (**l**) were analyzed by flow cytometry and quantified as a fraction of B cells. (**m**) NP-specific IgG titers. The dotted line indicates NP-specific titers in naive mice. *p<0.05, **p<0.001, ***p<0.0001 (two-tailed unpaired Student's *t* test). Data are pooled from four (**a–f**) five (**g–i**) or two (**j–m**) independent experiments with n=6-14 mice per group (mean ± s.e.m.).

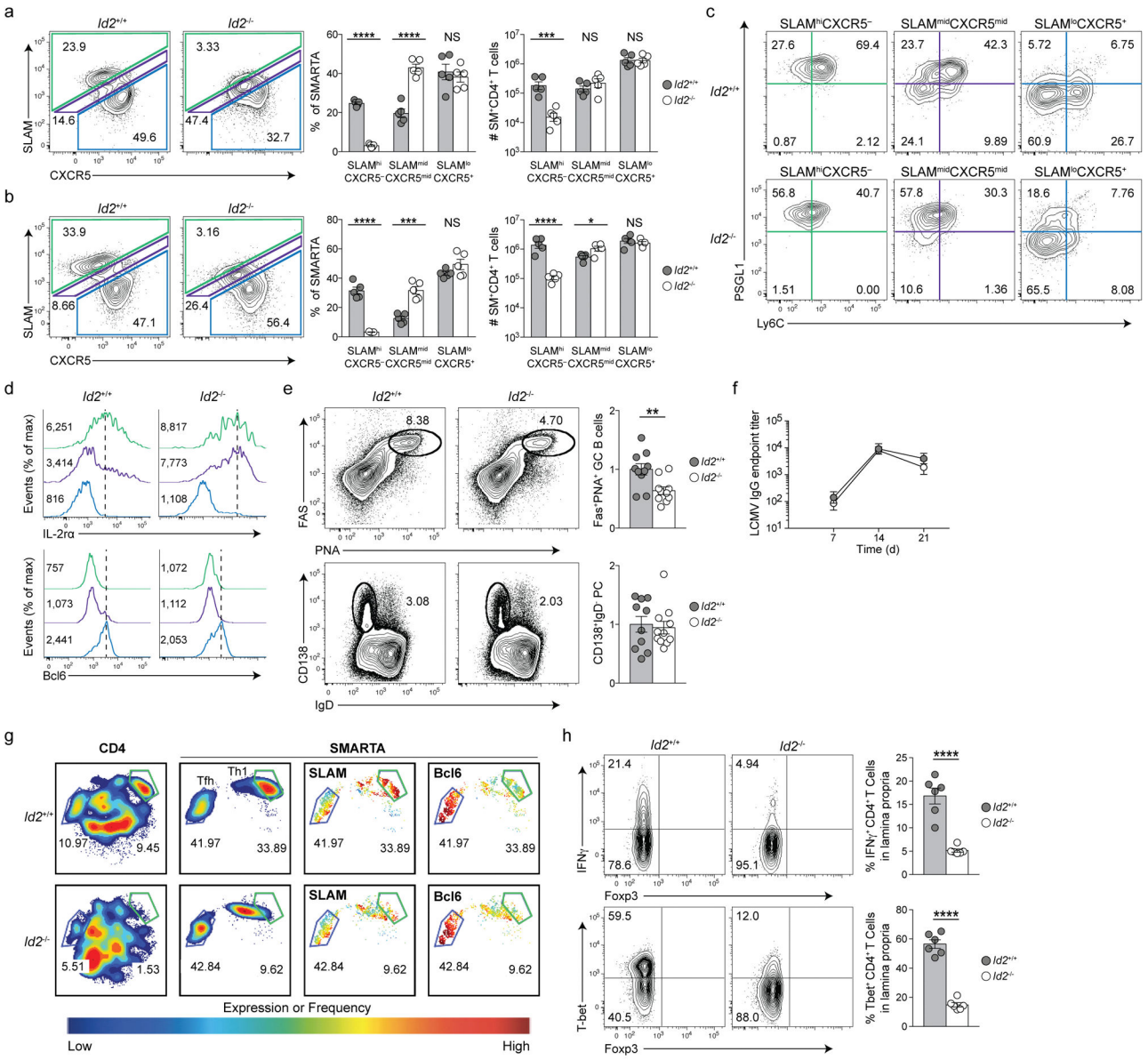

Figure 3. Id2 is necessary for the generation of T_H1 $CD4^+$ helper cells during infection

(**a–d**,**g**) *Id2*$^{+/+}$ CD4-Cre$^+$ (*Id2*$^{+/+}$) or *Id2*$^{fl/fl}$ CD4-Cre$^+$ (*Id2*$^{-/-}$) SMARTA $CD4^+$ T cells were analyzed 4 (**a**,**c**,**d**,**g**) or 7 (**b**) days after LCMV infection. (**a**,**b**) $SLAM^{hi}CXCR5^-$ (green), $SLAM^{mid}CXCR5^{mid}$ (purple) and $SLAM^{lo}CXCR5^+$ (blue) cells were analyzed (left panels) and quantified as a frequency of SMARTA $CD4^+$ T cells (middle panels) and total cell numbers (right panels). PSGL-1 and Ly6C (**c**) and IL-2Rα or Bcl6 (**d**) expression on the indicated subsets, histogram color (**d**) corresponds to the gates drawn in (**a**). (**e**,**f**) *Id2*$^{+/+}$ or *Id2*$^{-/-}$ cells were transferred into *Bcl6*$^{fl/fl}$ CD4-Cre$^+$ mice and analyzed 8 (**e**) days after LCMV infection. (**e**) Analysis and quantification of GC B cells (Fas^+PNA^+) or plasma cells ($CD138^+IgD^-$) as a normalized frequency of B cells. (**f**) LCMV-specific IgG titers at the indicated time points. (**g**) viSNE analysis of total splenic $CD4^+$ T cells (left panel) or SMARTA $CD4^+$ T cells (right panels), with visualization of SLAM and Bcl6 expression by

color gradient. (**h**) *Id2*$^{+/+}$ CD4-Cre^{+} or *Id2*$^{fl/fl}$ CD4-Cre^{+} mice were infected with *T. gondii* and analyzed 7 days after infection. Analysis and quantification of IFNγ, T-bet and Foxp3 expression by lamina propria CD4^{+} T cells. *p<0.05, **p<0.01, ***p<0.001, ****p<0.0001 (two-tailed unpaired Student's *t* test). Data are representative of two (**f,h**) or three (**a–d,g**) experiments, each with n= 5–10 mice per group, or are pooled from two (**e**) independent experiments each with n= 10 mice per group (mean ± s.e.m.)

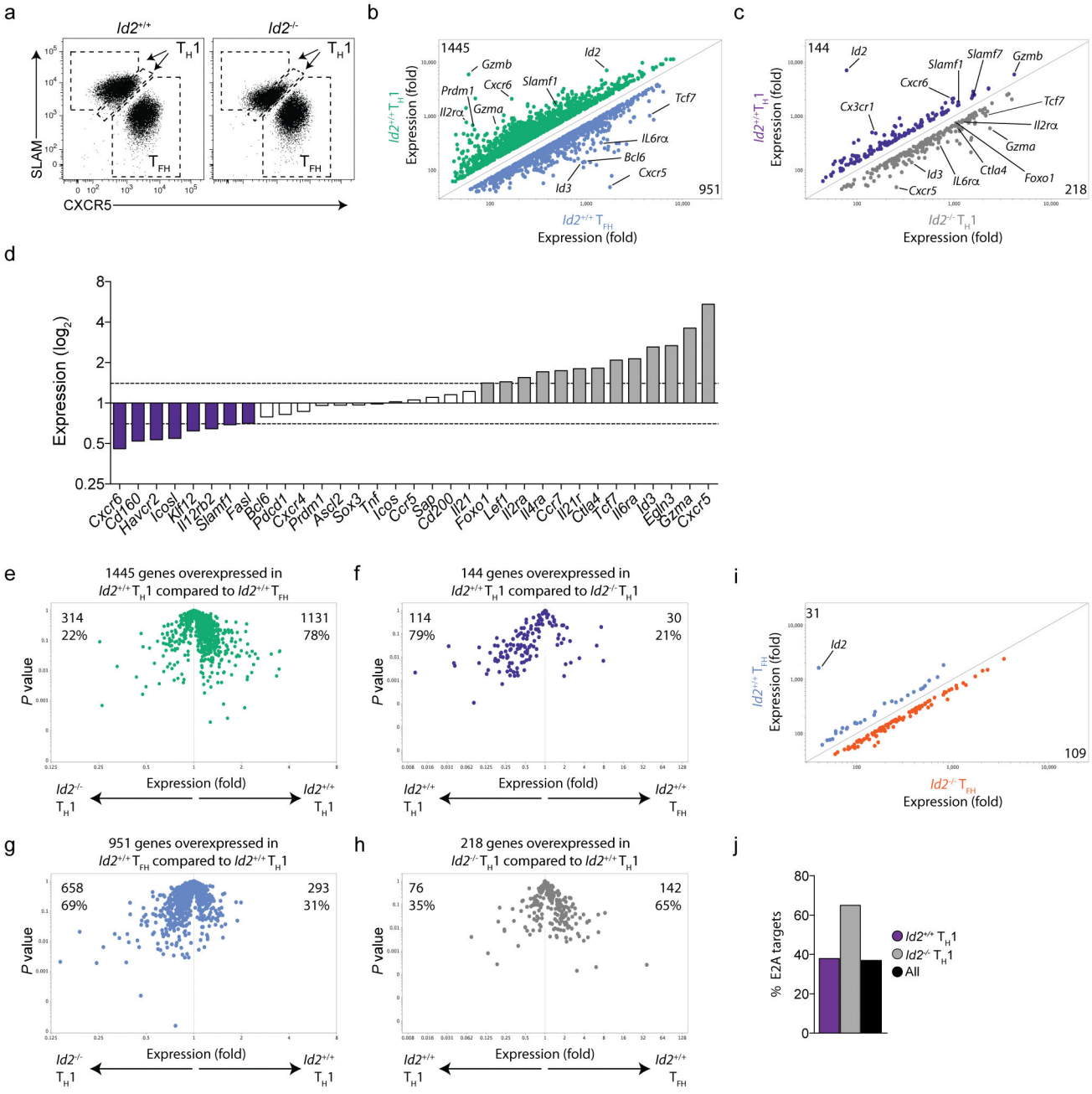

Figure 4. Increased E2A binding in the absence of Id2 regulates expression of key T helper genes

Id2$^{+/+}$ CD4-Cre^{+} (*Id2*$^{+/+}$) or *Id2*$^{fl/fl}$ CD4-Cre^{+} (*Id2*$^{-/-}$) SMARTA CD4^{+} T cells were transferred into B6 hosts and infected with LCMV. (**a**) Microarray analysis was performed on the indicated T_H1 and T_{FH} populations sorted 7 days after LCMV infection. (**b** and **c**) Comparisons between the indicated populations are shown as expression-by-expression plots with FC ≥1.4, CV ≤ 0.10 and expression ≥40. (**d**) Expression of putative E2A-target genes identified by ChIP-seq between *Id2*$^{+/+}$ T_H1 (purple) and *Id2*$^{-/-}$ T_H1 (grey). White bars indicate genes not significantly differentially regulated. (**e-h**) Volcano plots for the indicated data sets. (**e**) Differentially regulated *Id2*$^{+/+}$ T_H1 genes from *Id2*$^{+/+}$ T_H1 vs *Id2*$^{+/+}$ T_{FH} mean-

class expression (MCE) plot (**b**). (**f**) Differentially regulated *Id2*$^{+/+}$ T_H1 genes from *Id2*$^{+/+}$ T_H1 vs *Id2*$^{-/-}$ T_H1 MCE plot (**c**). (**g**) Differentially regulated *Id2*$^{+/+}$ T_{FH} genes from *Id2*$^{+/+}$ T_{FH} vs *Id2*$^{+/+}$ T_H1 MCE plot (**b**). (**h**) Differentially regulated *Id2*$^{-/-}$ T_H1 genes from *Id2*$^{-/-}$ T_H1 vs *Id2*$^{+/+}$ T_H1 MCE plot (**c**). (**i**) Comparisons between *Id2*$^{+/+}$ and *Id2*$^{-/-}$ T_{FH} are shown as expression-by-expression plots with FC ≥1.4, CV ≤0.10 and expression ≥40. (**j**) Frequency of differentially regulated genes (FC ≥1.4) between *Id2*$^{+/+}$ T_H1 and *Id2*$^{-/-}$ T_H1 populations, which are also E2A targets as indicated by E2A ChIP-seq. Black bar indicates the background frequency of E2A targets. Data are representative of 2 independent experiments each with n= 5 mice per group.

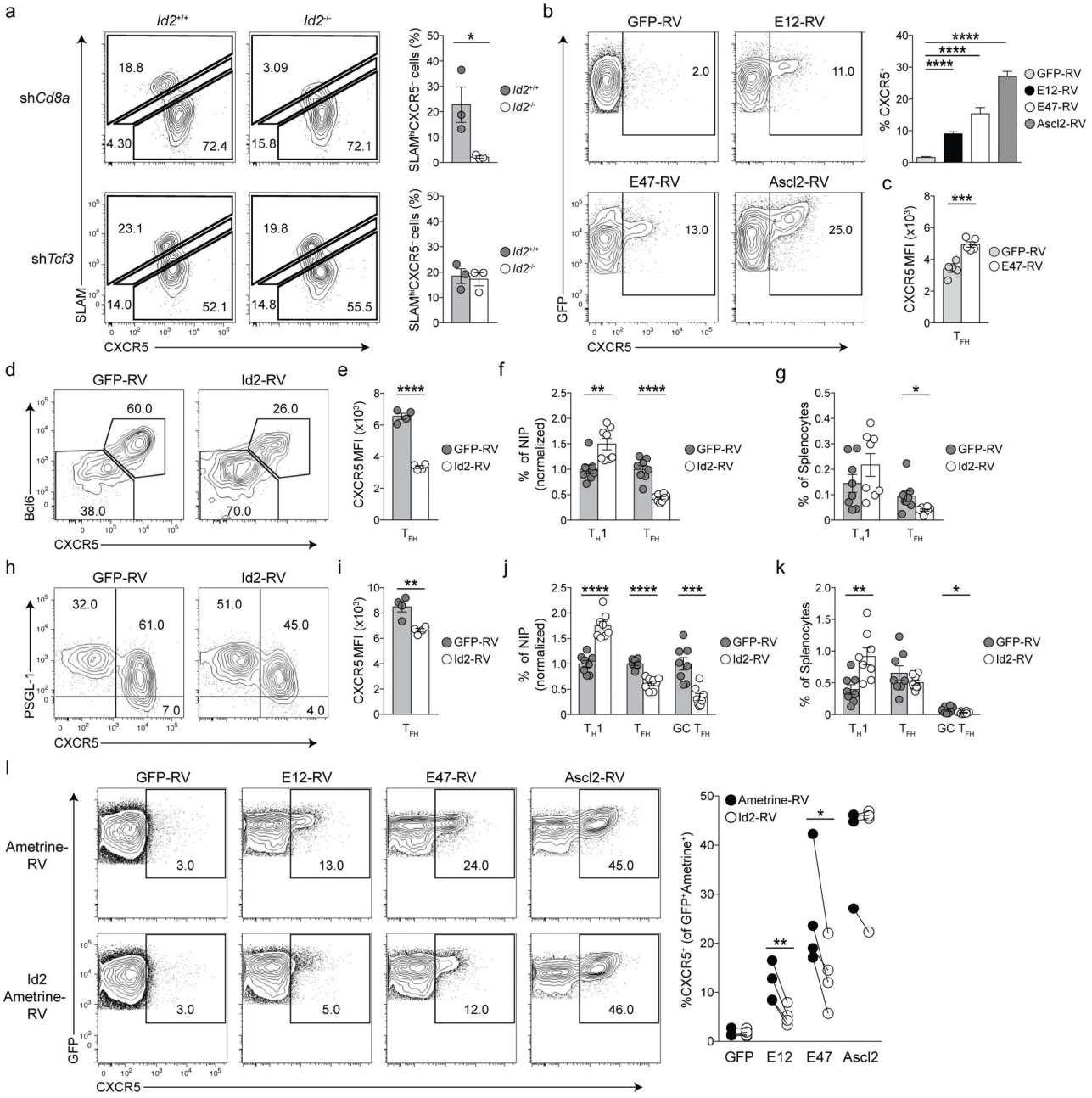

Figure 5. E proteins drive CXCR5 expression and inhibit T_H1 formation

(**a**) *Id2*$^{+/+}$ CD4-Cre^{+} (*Id2*$^{+/+}$) or *Id2*$^{fl/fl}$ CD4-Cre^{+} (*Id2*$^{-/-}$) SMARTA CD4^{+} T cells were transduced with the indicated shRNAmir-RV, transferred into B6 mice and analyzed 7 days after LCMV infection. T_H1 cells were analyzed by flow cytometry and quantified as a fraction of transduced SMARTA CD4^{+} T cells. (**b**) CXCR5 expression in GFP^{+} CD4^{+} T cells and pooled quantitation. (**c**) Quantitation of CXCR5 expression by RV^{+} SMARTA T_{FH} (CXCR5^{+}Bcl6^{+}) cells 3 days after LCMV. (**d–k**) RV transduced NIP CD4^{+} T cells were transferred into B6 mice and analyzed 3 (**d–g**) or 6 days (**h–k**) after LCMV infection. (**d–g**) T_{FH} (CXCR5^{+}Bcl6^{+}) and T_H1 (CXCR5^{-}Bcl6^{-}) differentiation was analyzed by flow

cytometry (**d**) and quantified as a fraction of NIP $CD4^+$ T cells (**f**) or total splenocytes (**g**). (**e**) Quantitation of CXCR5 expression in NIP T_{FH} ($CXCR5^+Bcl6^+$) cells. (**h–k**) T_H1 ($PSGL\text{-}1^+CXCR5^-$), T_{FH} ($CXCR5^+PSGL\text{-}1^+$) and GC T_{FH} ($CXCR5^+PSGL\text{-}1^-$) cell development was analyzed by flow cytometry (**h**) and quantified as a fraction of NIP $CD4^+$ T cells (**j**) or total splenocytes (**k**). (**I**) Quantitation of CXCR5 expression in NIP T_{FH} ($CXCR5^+SLAM^{lo}$) cells. (**l**) CXCR5 expression by GFP^+Ame^+ $CD4^+$ T cells and quantitation. *p<0.05, **p<0.01, ***p<0.001, ****p<0.0001(two-tailed unpaired (a–k) or paired (l) Student's *t* test). Data are representative of two (**a,c**), three (**d,e**) or four (**h,i**) independent experiments or pooled from two (**f,g,j,k**), four (**l**) or nine (**b**) individual experiments each with n= 3-8 mice per group (mean ± s.e.m.).

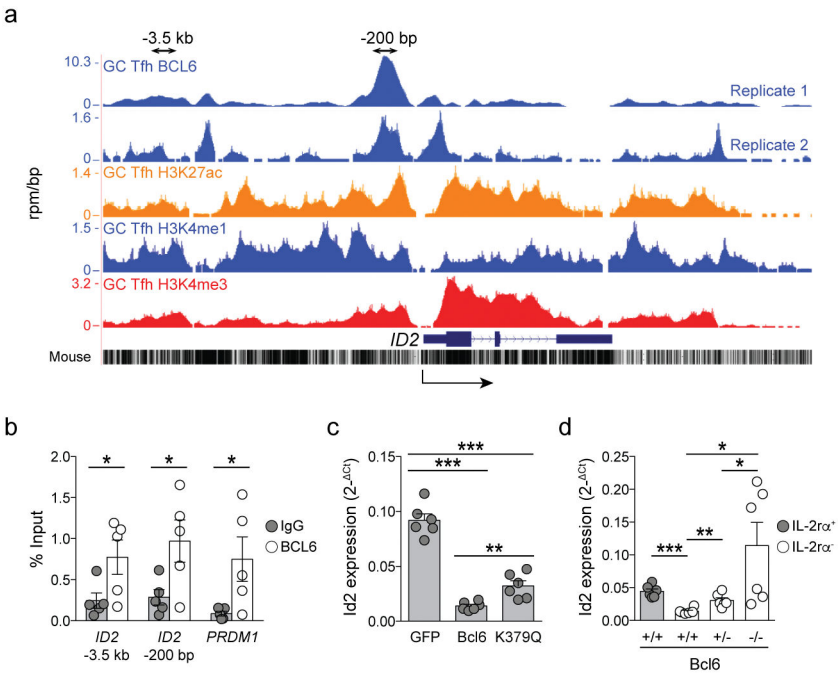

Figure 6. Bcl6 inhibits *Id2* expression

(**a**) BCL6, H3K27Ac, H3K4me1 and H3K4me3 density tracks of *ID2* in human GC T_{FH} cells. Arrows above the BCL6 tracks indicate primers used in ChIP-qPCR analysis. Sequence conservation with mouse is shown at the bottom. (**b**) PD-1^{hi} GC T_{FH} cells were isolated from human tonsil cells, chromatin was prepared and ChIP was performed for BCL6 at the indicated loci. (**c**) *Bcl6*$^{fl/fl}$ CD4-Cre^{+} SMARTA CD4^{+} T cells transduced with the indicated vectors were transferred into B6 mice. IL-2Rα^{+} SMARTA CD4^{+} T cells were sorted 3 days after LCMV infection and *Id2* expression was tested by qRT-PCR. (**d**) WT (*Bcl6*$^{+/+}$), *Bcl6*$^{fl/WT}$ CD4-Cre^{+} (*Bcl6*$^{+/-}$), *Bcl6*$^{fl/fl}$ CD4-Cre^{+} (*Bcl6*$^{-/-}$) SMARTA CD4^{+} T cells were transferred into B6 mice. IL-2Rα^{+} or IL-2Rα^{-} SMARTA cells were sorted and *Id2* expression was tested by qRT-PCR. *p<0.05, **p<0.01, ***p<0.0001 (two-tailed unpaired Student's *t* test). Data are pooled from two (**c,d**) or four (**b**) independent experiments, with n= 5 mice per group (**b**) (mean ± s.e.m.). For c and d, 3 mice were pooled to create a data point.